Journal of Neuroinflammation

RESEARCH

Open Access

Microglia in the aged brain develop a hypoactive molecular phenotype after surgery

Zhuoran Yin[1,2†], Anna K. Leonard[3†], Carl M. Porto[3], Zhongcong Xie[4,5], Sebastian Silveira[1], Deborah J. Culley[6], Oleg Butovsky[1,7] and Gregory Crosby[3,5*]

Abstract

Background Microglia, the resident immune cells of the brain, play a crucial role in maintaining homeostasis in the central nervous system (CNS). However, they can also contribute to neurodegeneration through their pro-inflammatory properties and phagocytic functions. Acute post-operative cognitive deficits have been associated with inflammation, and microglia have been implicated primarily based on morphological changes. We investigated the impact of surgery on the microglial transcriptome to test the hypothesis that surgery produces an age-dependent pro-inflammatory phenotype in these cells.

Methods Three-to-five and 20-to-22-month-old C57BL/6 mice were anesthetized with isoflurane for an abdominal laparotomy, followed by sacrifice either 6 or 48 h post-surgery. Age-matched controls were exposed to carrier gas. Cytokine concentrations in plasma and brain tissue were evaluated using enzyme-linked immunosorbent assays (ELISA). Iba1$^+$ cell density and morphology were determined by immunohistochemistry. Microglia from both surgically treated mice and age-matched controls were isolated by a well-established fluorescence-activated cell sorting (FACS) protocol. The microglial transcriptome was then analyzed using quantitative polymerase chain reaction (qPCR) and RNA sequencing (RNAseq).

Results Surgery induced an elevation in plasma cytokines in both age groups. Notably, increased CCL2 was observed in the brain post-surgery, with a greater change in old compared to young mice. Age, rather than the surgical procedure, increased Iba1 immunoreactivity and the number of Iba1$^+$ cells in the hippocampus. Both qPCR and RNAseq analysis demonstrated suppression of neuroinflammation at 6 h after surgery in microglia isolated from aged mice. A comparative analysis of differentially expressed genes (DEGs) with previously published neurodegenerative microglia phenotype (MGnD), also referred to disease-associated microglia (DAM), revealed that surgery upregulates genes typically downregulated in the context of neurodegenerative diseases. These surgery-induced changes resolved by 48 h post-surgery and only a few DEGs were detected at that time point, indicating that the hypoactive phenotype of microglia is transient.

Conclusions While anesthesia and surgery induce pro-inflammatory changes in the plasma and brain of mice, microglia adopt a homeostatic molecular phenotype following surgery. This effect seems to be more pronounced in aged mice and is transient. These results challenge the prevailing assumption that surgery activates microglia in the aged brain.

Keywords Microglia, Aging, Surgery, Neuroinflammation

†Zhuoran Yin and Anna K. Leonard have authors contributed equally.

*Correspondence:
Gregory Crosby
gcrosby@bwh.harvard.edu
Full list of author information is available at the end of the article

Background

Cognitive morbidity is one of the most common complications of surgery in older individuals. Nationally, one out of three surgical procedures is performed on a person aged 65 or older. Among those undergoing non-cardiac surgery, 20–60% develop delirium, which is an acute confusional state, while 10–15% exhibit subtle but persistent cognitive decline postoperatively [1–3]. This cognitive morbidity is associated with adverse outcomes, such as poor quality of life, greater mortality, and potential acceleration of decline towards dementia [4–8]. Although the pathogenesis of this cognitive dysfunction remains uncertain and is likely multifactorial, postoperative inflammation within the central nervous system (CNS) has emerged as a leading candidate [9].

Surgery is a potent trigger of systemic aseptic inflammation and increases damage-associated and proinflammatory molecules in the circulation. These molecules, in turn, communicate with the CNS via vagal cholinergic afferents and/or by direct entry [10, 11] to induce a cascade of inflammatory events in the brain. In preclinical models of orthopedic or abdominal surgery, inflammatory mediators such as IL-1β, TNFα, IL-6, and CCL2 are elevated in the hippocampus after surgery and microglia undergo morphological changes often attributed to activation [12–22]. This surgery-induced neuroinflammation is associated with cognitive impairment and some studies demonstrate that pharmacologic or genetic interventions that attenuate or block this inflammatory response prevent the cognitive dysfunction [12, 13, 23–25]. Likewise, in humans, postoperative delirium and persistent cognitive impairment are associated with increases in proinflammatory mediators such as IL-6, CCL2, and YKL-40 in both plasma and cerebrospinal fluid [26–29]. These findings align with evidence that neuroinflammation plays a role in the pathogenesis of cognitive decline associated with age and neurologic diseases [14, 30–39]. Thus, while not all studies agree, considerable evidence supports the concept that CNS inflammation contributes to surgery-induced cognitive morbidity. The cells responsible for this pro-inflammatory state are not fully understood; however, microglia, the resident immune competent cells of the CNS, have been strongly implicated [12, 13, 23–25, 40].

Microglia play a crucial role in immune surveillance and maintaining CNS homeostasis, but also contribute to neurodegeneration via their pro-inflammatory properties and phagocytic activities [41–43]. Preclinical studies indicate that surgery increases the expression of microglial products such as IL-1β, TNFα, IL-6 and CCL2 in the brain. Morphological changes in these cells, which may signify activation, are observed through staining for the myeloid cell marker ionized calcium binding adaptor protein (Iba1). Some preclinical studies also show that inhibiting or partially depleting microglia pharmacologically can mitigate postoperative cognitive impairment [13, 23]. Nonetheless, there are reasons to be uncertain about the impact of surgery on microglia. Many studies have used young animals [44], which is problematic because microglial density, phenotype, and function change substantially with age and the cognitive morbidity of surgery is mainly a complication in geriatric patients. Furthermore, Iba1 is not specific for microglia, and cellular morphology is an unreliable index of the microglial activation state [37, 45–47]. Adding to the complexity is the fact that microglia, which account for 10–15% of the cells in the brain, exhibit considerable molecular and functional diversity [47]. Some phenotypes contribute to neurodegeneration, whereas others are essential for maintaining neuronal homeostasis [42, 47, 48]. They are also highly dynamic cells. Microglial phenotypes change with age [toward an activated response- or disease-associated/neurodegenerative phenotype (DAM, MGnD, respectively)] and shift rapidly in response to insults [49–52], an important consideration in the context of the acute trauma of geriatric surgery. Further, each microglial phenotype has a distinct molecular signature that strongly predicts its function [47, 49–52]. Yet, traditional approaches such as Iba1 immunohistochemistry cannot discriminate between the various microglial phenotypes and no studies have investigated the microglial response to surgery at the transcriptome level. Moreover, not all animal studies agree [53, 54], and the only two studies that examined the microglial activation state in the human brain after surgery demonstrate microglial hypoactivity—not activation—in the first postoperative days or weeks [55, 56].

We hypothesized that surgery triggers microglial activation, particularly in aged animals, and transforms them into a pro-inflammatory phenotype. To test this hypothesis, we analyzed the microglial response to surgery using immunohistochemistry, qPCR for selected transcripts, and bulk RNA sequencing of the microglial transcriptome in young and aged mice. Surprisingly, the results contradict our initial expectations and demonstrate that microglia undergo minimal post-surgical changes in young mice and develop a hypoactive phenotype, albeit only transiently, in the aged.

Materials and methods

Animals

The animal use procedures were approved by the Institutional Animal Care and Use Committee (IACUC) at Brigham and Women's Hospital (BWH). Male C57BL/6 mice at 3–5 months old ("young") and 20–22 months old ("old") were obtained from Charles River Laboratories

(old mice obtained from the NIA Aged Rodent Colony at Charles River) and housed at the BWH animal Center. B6.129P2(Cg)-*Cx3cr1*$^{tm2.1(cre/ERT)Litt}$/WganJ (Cx3cr1^{CreERT2}) [57] mice were purchased from the Jackson Laboratory. Generation of *Apoe*$^{fl/fl}$ mice has been described previously [58] and these mice were crossed with Cx3cr1$^{CreERT2/+}$ mice to target *Apoe* in long-lived myeloid cells. Colony room conditions were maintained at 18–23 °C and 40% to 60% humidity, with lights set to a 12-h light/dark cycle. Experiments were performed as outlined when mice were within 3–5 or 20–22 months of age.

Conditional knock out of apoe

To induce elimination of Apoe in microglia, Cx3cr1$^{creERT2/+}$:*Apoe*$^{fl/fl}$ and Cx3cr1$^{+/+}$:*Apoe*$^{fl/fl}$ (age-matched control) mice were intraperitoneally (i.p.) injected at 6 weeks of age with 150 mg of tamoxifen (Sigma Aldrich, T5648-5G) dissolved in corn oil per kg body weight per day for two consecutive days.

Experimental procedure

Mice allocated to surgery were placed in an induction chamber (t = 0 h [h]) containing 1.2% isoflurane (Patterson Veterinary #78,938,441) vaporized in an atmospheric gas mixture of 30% oxygen balanced with nitrogen ("carrier gas"; AirGas #Z02NI7012000310). The anesthetic concentration in the chamber was monitored with an infrared agent analyzer (Vamos, Drager US, Telford, PA) and body temperature was monitored and maintained at 37 ± 0.5 °C with a heating pad (Right Temp Jr, Kent Scientific, Torrington, CT). Approximately 15 min post-induction, mice were removed from the chamber and isoflurane was administered by nose cone while an abdominal laparotomy was performed. The abdomen was shaved and swabbed with 70% ethanol and 10% povidone-iodine. Bupivacaine (0.5 ml of 0.25%; Patterson Veterinary #78,904,881) was injected subcutaneously along the midline of the abdomen from just below the diaphragm to the pelvis. Meloxicam (Alloxate; 2 mg/kg; Patterson Veterinary #07–893-7565) was also administered subcutaneously. A 1.5 cm incision was made along the midline, and the bowels were exteriorized and probed with a blunt instrument for approximately 5 min. The bowels were then returned to the abdomen and the incision was closed in layers with sutures. The total duration of the procedure was approximately 20 min, after which the animals were returned to the anesthetic chamber for the remainder of the 2-h anesthesia period. At the end of the 2-h exposure, the isoflurane was discontinued, and the chamber was flushed with 30% oxygen. Mice remained on the heating pad until they regained spontaneous locomotor activity, at which point they were returned to the home cage. Age-matched controls were treated identically except that they had no anesthesia or surgery. Controls were placed in identical chambers filled with carrier gas alone for 2 h and received bupivacaine and meloxicam in the same manner and dose as the surgery groups. Mice were euthanized either 6 or 48 h after the start of anesthesia or administration of carrier gas; animals in the 48 h groups were returned to the animal facility until sacrifice and received a supplemental dose of meloxicam at 24 h after the treatment.

Euthanasia and sample collection

Mice were deeply anesthetized with 3–4% isoflurane. Up to 1 ml of blood was quickly drawn from the heart with a 28 g insulin syringe (Owens & Minor # 5,858,044,281) and then mice were perfused intracardially with 20 ml of ice-cold 1X phosphate-buffered saline (PBS). The brain was removed, dissected on ice, frozen at − 80 °C and processed according to the intended analysis. The blood was placed in a 1.2 ml EDTA tube (Fisher Scientific #NC0826920) and centrifuged at 2000 RPM for ten minutes. Plasma was separated and spun again at 4000 RPM for ten minutes, then decanted from the pellet and stored at − 80 °C.

Analysis of protein expression

For quantification of plasma proteins, plasma was thawed to room temperature and run on an ELISA (IL-6 Quantikine Mouse ELISA; R&D Systems #M6000B or CCL2 Quantikine Mouse ELISA, R&D Systems #MJE00B) according to manufacturer's instructions.

For analysis of brain tissue protein expression, one hemisphere of the frontal cortex or hippocampus was dissected, placed in a 1.5 ml microcentrifuge tube, flash frozen in absolute ethanol chilled with dry ice, and stored at − 80 °C until homogenization. Prior to homogenization, tissue samples were thawed on ice. A roughly equal volume of 0.5 mm zirconium oxide beads was added, with 300 ul lysis buffer composed of Tissue Protein Extraction Reagent (T-per; ThermoFisher #78,510) supplemented with 2.5X Halt protease inhibitor cocktail (Life Technologies #87,786) and Halt phosphatase inhibitor cocktails (Life Technologies #78,420). Samples were homogenized in 10 s intervals (Bullet Blender, Next Advanced) set to speed 8, with ice applied in between each interval, until sample was visually homogenous (approximately 30 s total). To clear debris, samples were spun at 14,000 *g for 6 min and supernatant was transferred to clean microcentrifuge tubes. A portion was reserved for total protein content quantification by the Pierce BCA Protein Assay Kit (Life Technologies #23,227), according to the manufacturer's instructions. The remainder was aliquoted and stored at − 80 °C until ELISA quantification. Brain

tissue CCL2 (Quantikine ELISA kit #MJE00B; R&D Systems) and IL-6 (IL-6 Mouse High Sensitivity ELISA kit #50,246,676; ThermoFisher) were quantified by ELISA according to manufacturers' instructions. Cytokine concentrations in tissue were normalized to the total protein concentration (pg/mg).

Immunohistochemistry (IHC)

Microglia were labeled with ionized calcium binding adaptor protein (Iba1) for immunohistochemistry. One hemisphere of the brain was drop-fixed in 4% paraformaldehyde for 24 h, followed by 48 h in 30% sucrose for cryoprotection. After cryoprotection, hemispheres were flash-frozen in 2-methylbutane at − 20 °C. Frozen brains were coated in optimal cutting temperature (OCT) compound (Sakura FineTek #4583) and sectioned at 40 µm on the sagittal plane with a cryostat. Sections were stored at 4 °C in 1X PBS with 0.01% sodium azide until staining. Sections were washed in 1X PBS, then incubated for 1 h in blocking buffer (5% normal donkey serum, 0.3% Triton-X 100 in 1X PBS). Primary antibody (rabbit anti-Iba1, Wako Chemicals #019–19794, 1:1000 in blocking buffer) was added and incubated overnight at room temperature. Sections were washed in 1X PBS, then incubated in secondary antibody (AlexaFluor 488 donkey anti-rabbit; Invitrogen #A-21206; 1:500 in blocking buffer) for 2 h at room temperature. Sections received a final wash in 1X PBS, then were stored at 4 °C until mounting onto Superfrost Plus microscope slides (FisherBrand #12–550-15). Coverslips were applied with Vectashield HardSet antifade mounting medium with DAPI (Vector Laboratories #H-1500-10).

Imaging and quantification

Images were acquired at 10X magnification on a Keyence BZ9000 microscope. Image quantification was performed in Fiji-ImageJ. For each image, the region of interest (ROI) was outlined, and the background was excluded using the threshold function. The total selection area, area above the threshold, and mean gray value of pixels above the threshold were quantified with the Measure function. The number of $Iba1^+$ cells was quantified with the 3D Objects Counter Function. Percent area stained was computed as the area above the threshold divided by the total area of the ROI. Cell density was calculated as the number of cells divided by the total area of the ROI. Three sections were imaged per region per mouse; individual data points for each mouse represent the average of the three sections.

Fluorescence-activated cell sorting

For analysis of the microglial transcriptome, brains were dissected into two samples: the total hippocampi (including left and right hippocampus), and one whole hemisphere without the hippocampus. Immediately after dissection, the samples were placed in ice-cold Hanks' Balanced Salt Solution (HBSS). The brain tissue was mechanically dissociated with a homogenizer to form a single cell suspension, then centrifuged at 800G at 23 °C for 25 min in a 37%/70% Percoll Plus gradient (GE Healthcare #17–5445-02), with an acceleration of 3 and a deceleration of 1. Mononuclear cells were taken from the interface layer. The population of $Ly\text{-}6C^-CD11b^+FCRLS^+$ microglial cells was stained and labeled with anti-FCRLS-APC (1:1000, clone 4G11) [59], anti-mouse CD11b-PeCy7 (1:300, eBioscience #50–154-54), and anti-mouse Ly-6C-PerCP/Cy5.5 (1:300, Biolegend #123,012), a method that captures the entire microglia population and also excludes infiltrating myeloid cells because they do not express FCRLS [52, 59]. Cells were then sorted using BD FACSAria™ II (BD Bioscience) or MoFlo Astrios (Beckman Coulter Life Sciences) cell sorter. One aliquot of one thousand cells was reserved for RNA-seq. The remainder was used for qPCR. For practical reasons (i.e. evening availability), sorting was conducted on two machines but we used the same staining and gating strategy across all samples, and all control and surgery samples from a given time point (6 or 48 h sacrifice) were processed on the same machine.

qPCR

For analysis of microglial inflammatory marker expression, RNA was extracted from FACS-isolated microglia using the RNeasy Plus Micro Kit (Qiagen # 74,034), according to the manufacturer's instructions. RNA content in the final elution was quantified by NanoDrop (Thermo Scientific), then diluted to 3 ng/ul in nuclease-free water. Diluted RNA was mixed with an equal volume of 2X High-Capacity cDNA Reverse Transcription master mix with RNase inhibitor (Applied Biosystems #4,374,966; final concentration 1X) in 0.2 ml Rnase-free PCR tubes. Samples were incubated at 25 °C for 10 min, 37 °C for 2 h, and 85 °C for 5 min in a thermal cycler, then stored at 4 °C until further use. For quantitative PCR, 1.5 ul cDNA was mixed with 0.75 ul nuclease-free water, 0.25 ul primer, and 2.5 ul TaqMan Fast Universal PCR MasterMix (2X), no amperase (Applied Biosystems #4,352,042) in a 384-well plate. Primers included *Gapdh* (housekeeping gene; ThermoFisher Mm99999915_g1), *Apoe* (ThermoFisher Mm01307192_m1), *Tgfbr1* (ThermoFisher Mm00436964_m1), *Clec7a* (ThermoFisher Mm01183349_m1), *Il6* (ThermoFisher Mm00446191_m1), and *Il1β* (ThermoFisher Mm99999061_mH). Each sample was processed in triplicate. Cycle threshold of *Apoe, Tgfbr1, Clec7a, Il6,* and *Il-1β* was normalized to

Gapdh, then to the average expression of the young control group (ΔΔCt).

RNAseq

For bulk analysis of the microglia transcriptome, 1000 isolated Ly6C^{-}CD11b^{+} FCRLS^{+} microglia per sample were lysed with 5 ul of Buffer TCL (Qiagen #1,070,498) containing 1% 2-mercaptoethanol, then refrozen on dry ice and transported to the Broad Institute. RNA quality control, SmartSeq2 library preparation [60] and quality control, and sequencing were performed by the Broad Institute Genomics Platform; all samples passed QC measures. RNA was first purified using 2.2X RNA-SPRI beads (Beckman Coulter Genomics) and eluted into a mix of 3′ RT primer, dNTP mix Rnase inhibitor and trehalose to prime the samples for reverse transcription. A solution of 5 × Maxima RT buffer, trehalose, $MgCl_2$, TSO, RNase Inhibitor, and Maxima RNaseH- minus RT was added to facilitate both first and second strand cDNA synthesis. Samples then underwent PCR pre-amplification using HiFi HotStart ReadyMix (Kapa) and ISPCR Primer, followed by a 0.8X SPRI bead cleanup. cDNA concentration was assessed using Quant-iTTM PicoGreenTM dsDNA Assay Kit (ThermoFisher Scientific) and normalized to 0.25 ng/ul. cDNA libraries were constructed using a Nextera XT DNA Library Preparation kit (Illumina, San Diego, CA). Tagmentation was performed to fragment the cDNA and add adapter sequences. After the tagmentation reaction was neutralized, libraries were PCR amplified with Illumina p7 and p5 index adapters. cDNA libraries were then pooled and underwent a final 0.9X SPRI bead clean up. Library quality was assessed using an Agilent Bioanalyzer trace. Final libraries had a size of 500 bp. Pooled libraries were normalized to 2 nM and denatured using 0.1 N NaOH. Flowcell cluster amplification and sequencing were performed according to the manufacturer's protocols on a NextSeq 500 (Illumina) using a High Output v2 kit to generate 2 × 38 bp reads. Alignment and counting of FASTQ files were performed using the bcbio-nextgen Bulk RNA-seq analysis pipeline provided by the Bioinformatics Core at Harvard Chan School of Public Health (https://bcbio-nextgen.readthedocs.io/en/latest/contents/bulk_rnaseq.html; accessed June 2022). This pipeline includes alignment to the mouse genome (mm10) with hisat2 [61], and gene-level expression counts using Salmon [62], and quality control by fastQC (http://www.bioinformatics.babraham.ac.uk/projects/fastqc/) and multiQC [63]. Gene expression data were divided into four data sets: "hemisphere, 6 h"; "hemisphere, 48 h"; "hippocampus, 6 h"; and "hippocampus, 48 h". Low abundance genes were defined as those with a mean of < 5 reads/sample and filtered out. Differential gene expression was calculated with the DESeq2-Wald test (v1.36.0) with Benjamini–Hochberg correction for multiple comparisons in R (v4.2.1). Contrasts tested included the main effect of age (old control vs. young control mice) andthe main effect of treatment (young surgery vs. young control mice, old surgery vs. old control mice). Significant differentially expressed genes (DEGs) were defined as those with Benjamini–Hochberg adjusted p-values (False Discovery Rate; FDR) less than 0.2 and a log2 Fold Change (log2FC) greater than |0.58|. Heatmaps were generated using the pheatmap R package (v1.0.12).

Statistical analysis

Group differences in ELISA, IHC, and qPCR measures were analyzed by two-way ANOVA (factors: Age and surgery; alpha = 0.5) and graphs were generated in GraphPad Prism 9.3.1. Data are shown as individual values with the mean ± one standard deviation (SD). If the age x treatment interaction was significant, post-hoc testing was performed with Šídák's multiple comparisons test to assess the effect of surgery within old mice and young mice separately.

Pathway analysis

Differentially expressed genes were used to detect the pathways associated with biological process. Differentially expressed genes with corresponding fold changes and adjusted p values were applied to Ingenuity pathway analysis (IPA, https://digitalinsights.qiagen.com/products-overview/discovery-insights-portfolio/analysis-and-visualization/qiagen-ipa/). In IPA, canonical pathways and biological functions were tested for generating biological networks as described previously [59].

Comparison to published RNAseq datasets

Previous studies have published SmartSeq2 profiles of microglial gene expression associated with neurodegenerative disease (i.e. Neurodegenerative microglia (MGnD) [52]; Disease-Associated Microglia (DAM) [49]. To assess how closely the profile of microglia post-surgery matches that of disease-associated microglia, we compared the fold-change of DEGs that overlapped between our datasets and previously published gene sets.

Results

Surgery increases markers of inflammation in plasma and brain

The experimental timeline is depicted in Fig. 1. We first assessed the level of inflammation in both the periphery and the brain after surgery by measuring the concentrations of Interleukin 6 (IL-6) and CC motif chemokine ligand 2 (CCL2) in plasma and brain homogenate by ELISA (Fig. 2a, b). Plasma IL-6 and CCL2 significantly

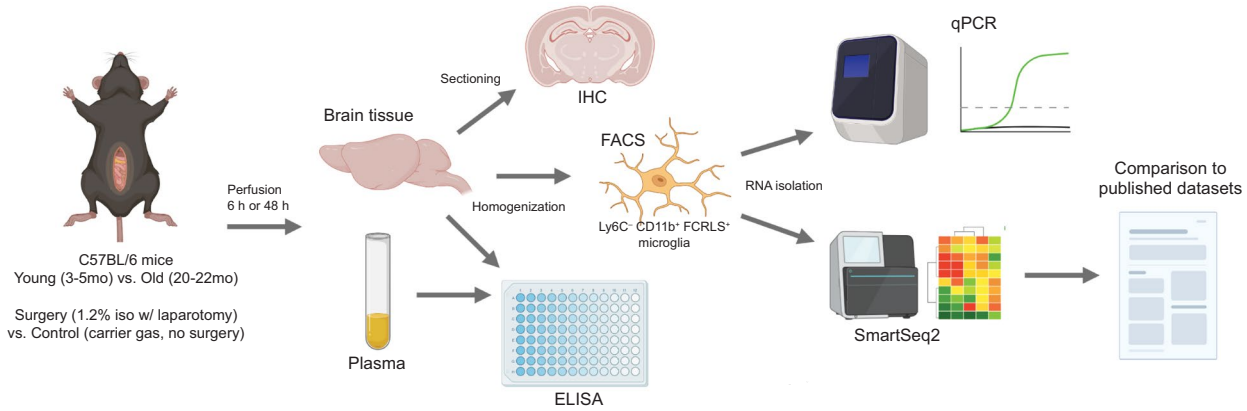

Fig. 1 Schematic of experimental design. Young (3–5 months old) or old (20–22 months old) male C57BL/6 mice received a 2-h exposure to 1.2% isoflurane and a 15-min abdominal laparotomy; age-matched controls received 2 h of carrier gas alone. Perfusions were performed at 6- or 48-h post-induction of anesthesia. Plasma was collected for cytokine ELISA. Brain tissue was harvested for thin sectioning and evaluation of microglial phenotype by IHC, and for isolation of microglia by FACS and subsequent analysis by qPCR or RNAseq. RNAseq datasets were compared to previously published data on MGnD and DAM transcriptomic phenotypes. Created with Biorender.com

increased 6 h after the surgery in both young and old mice compared to age-matched non-surgery controls (Fig. 2a). By 48 h after surgery, plasma IL-6 remained elevated, but this was only observed in old mice ($P < 0.0001$, Fig. 2b). There was no effect of age or treatment on IL-6 in the brain at either timepoint (Fig. 2a, b). In the frontal cortex, CCL2 was elevated in old mice at 48 h, while surgery had no effect. In contrast, there was a main effect of both age and surgery on CCL2 in the hippocampus at both 6 h and 48 h, as well a significant interaction between age and surgery. Hippocampal CCL2 was significantly elevated by surgery in old but not young mice at both 6 h ($P = 0.0013$) and 48 h ($P = 0.0001$) (Fig. 2a, b).

Surgery induces minimal changes in microglial morphology

Next, we evaluated age- and surgery-induced changes in Iba1$^+$ cells in the hippocampus by immunohistochemistry. Old control mice had more Iba1$^+$ cells in the CA3 and DG compared to young controls, as well as a greater percent area stained in the CA3 and DG at 48 h (Fig. 2c–f). Mean gray value was also higher in the old controls in DG but only in the 6 h group. In contrast to the clear effect of age, there were no post-surgical changes in the number or morphology of Iba1$^+$ cells (Fig. 2c–f).

Age and surgery produce opposing changes in microglial inflammatory markers

We isolated microglia using a well-established flow cytometry protocol as previously described [52] for analysis of various genes by qPCR. Previous work has characterized MGnD by upregulation of some inflammatory molecules such as *Apoe*, C-type lectin-like domain containing 7A (*Clec7a*), and Interleukin 1 beta (*Il1b*), and downregulation of homeostatic markers such as Transforming growth factor-beta receptor type 1 (*Tgfbr1*) and Purinergic Receptor P2Y12 (*P2ry12*) [49]. Here, we measured *Tgfbr1*, *Clec7a*, *Apoe*, *Il6*, and *Il1b* mRNA by qPCR in microglia isolated from the hippocampus or hemisphere 6 h or 48 h after surgery (Fig. 3a, b and Fig. S1).

Consistent with a neurodegenerative phenotype, *Tgfbr1* expression was lower in microglia from old than young control mice in both the hippocampus and hemisphere whereas *Clec7a* expression was higher. Surgery increased the expression of *Tgfbr1* in microglia of the young group at 6 h postoperatively (Fig. 3a), whereas it decreased the expression of *Clec7a* from microglia of the old group in both regions at that time (Fig. 3b). The surgery-induced changes in both *Tgfbr1* and *Clec7a* were transient and had resolved by 48 h postoperatively. Microglial expression of *Apoe, Il6* and *Il1b* also differed by age such that the expression of the genes was higher in cells from old compared to young control mice in the hippocampus and hemisphere (Fig. S1). However, other than an increase in *Il6* in the microglia of young mice, surgery had no effect on these genes in either age group (Fig. S1). Together, these data confirm previous reports that microglia develop a neurodegenerative molecular signature with age. Contrary to our expectation, however, the data suggest that surgery promotes development of a homeostatic phenotype rather than a proinflammatory one.

Surgery downregulates the inflammatory transcriptome of microglia in old mice

We then used Smartseq2 RNA sequencing (RNAseq) to determine broader transcriptional changes in

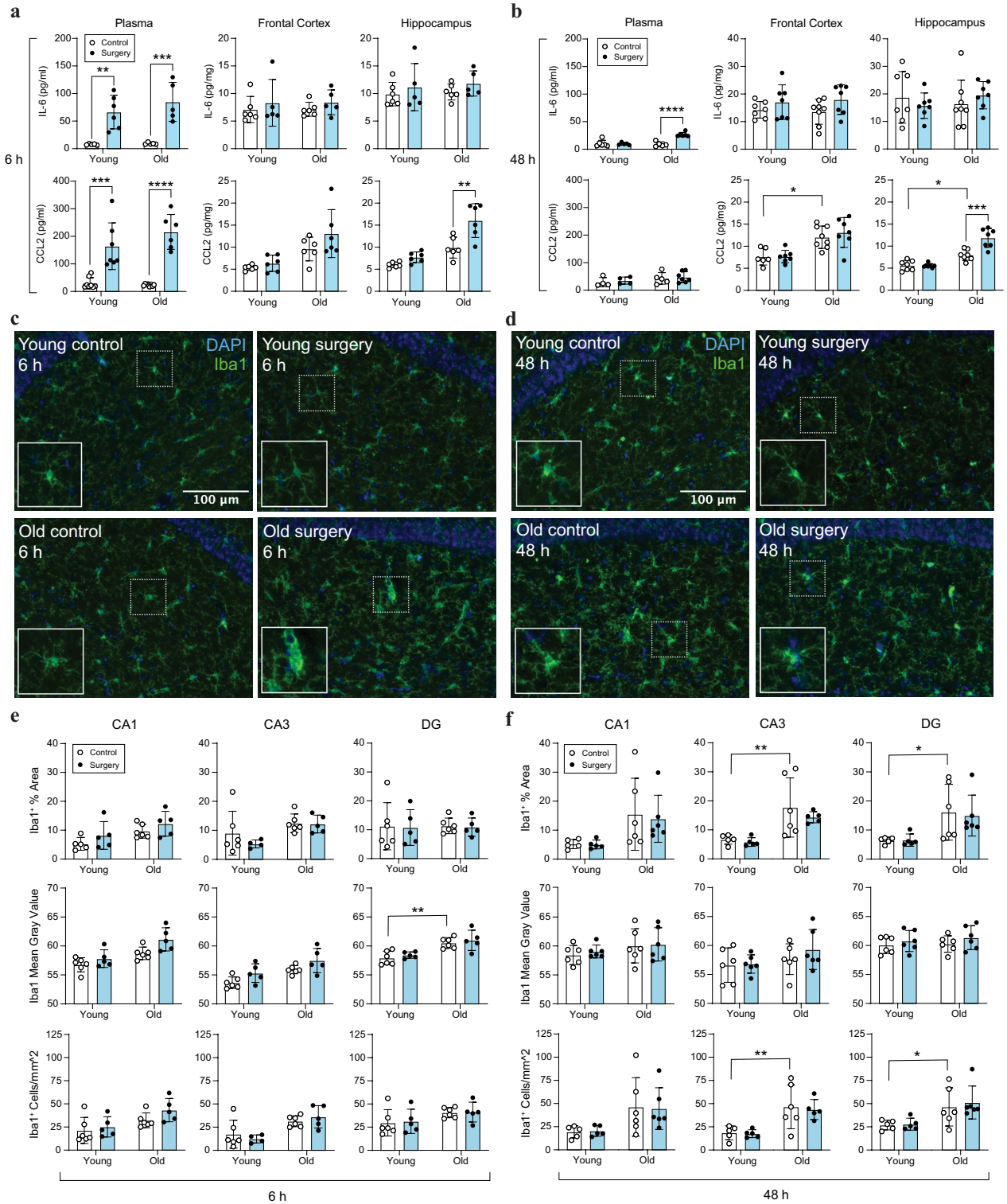

Fig. 2 Surgery induces systemic and CNS inflammation. **a**, **b** IL-6 and CCL2 were quantified by ELISA in the plasma, frontal cortex, and hippocampus of young and old mice 6 h (**a**) and 48 h (**b**) after surgery. **c** and **d**. 10 × microscopic images of Iba1$^+$ cells in the hippocampus (CA1) of young and old mice 6 h (**c**) or 48 h (**d**) after surgery. **e**, **f** Quantification of Iba1 immunohistochemistry (% area stained; mean gray value, and # of cells) in the CA1, CA3, and DG of the hippocampus 6 h (**e**) and 48 h (**f**) after surgery. Scale bars: 100 µm. Data are mean ± SD for 5–7 animals per group. Main effects calculated by two-way ANOVA, Šídák's multiple comparisons test. *$P < 0.05$; ***$P < 0.001$; **** $P < 0.0001$

microglia induced by surgery. The number of differentially expressed genes (DEGs) between surgery and control mice, categorized by age, region, and timepoint are shown in Fig. 3c. There were numerous DEGs 6 h after surgery and substantially more occurred in the microglia of old than young mice; by 48 h after surgery there were far fewer in both age groups (Fig. 3c). Therefore, we focused on the 6 h timepoint. Heatmaps of gene counts for DEGs from hemisphere and hippocampus are shown for young (Fig. 3d) and old mice (Fig. 3e). The expression of genes related to neuroinflammation, such as nuclear factor kappa B subunit 2 (*Nfkb2*), RELB proto-oncogene (*RelB*), and pro-inflammatory cytokine interleukin-6 signal transducer (*Il6st*), was reduced after surgery in the microglia of both young and old mice (Fig. 3d, e). *Nfkb2* encodes the precursor protein for nuclear factor κb (NF-κb), which acts as an activator of genes involved in inflammatory diseases. *RelB*, one of the noncanonical NF-κB members, mediates chemokine gene induction [64], and *Il6st* is upregulated in transgenic AD mice [65]. Meanwhile, microglial expression of some anti-inflammatory and homeostatic genes including Suppressor of cytokine signaling 3 (*Scos3*), an anti-inflammatory molecule that suppresses cytokine signaling and inflammatory gene expression [66], and DNA damage-inducible transcript 4 (*Ddit4*), a regulator of cell growth, proliferation, and survival [66], increased after surgery (Fig. 3d).

We next conducted a canonical pathway analysis of changes in old mice, as the small number of DEGs in the young mice prevented us from doing so in that age group. Ingenuity Pathway Analysis (IPA) revealed enhanced activity in the Signal transducer and activator of the transcription 3 (STAT3) pathway, HIF1a signaling, and FcgR-mediated phagocytosis in microglia from the hemisphere of old mice after surgery (Fig. 3f). This is noteworthy because the STAT3 pathway, including Insulin like growth factor 1 receptor (*Igf1r*), Fibroblast growth factor (*Fgf*), and Transforming growth factor beta-1 (*Tgfb1*), mediates the anti-inflammatory response [49]. Conversely, the Reactive Oxygen Species (ROS) and High mobility group box 1 (HMGB1) signaling pathways, which are both implicated in neuroinflammation, were downregulated after surgery in microglia from the hemisphere of old animals (Fig. 3f) as were pathways involved in neuroinflammation and dendritic cell maturation in microglia from the hippocampus of old mice after surgery (Fig. 3g).

Decreased expression of DAM and MGnD markers after surgery in aging brain

To further elucidate the phenotypic changes in microglia after surgery, we conducted a comparative analysis of the DEGs from our datasets with those published for disease associated microglia (DAM) and neurodegenerative microglia (MGnD) [49, 52] (Fig. 4). In the hemisphere, 93 DEGs affected by surgery in old mice and 27 from young mice were also present in the DAM profile. Ten of those genes overlapped between young and old mice (Fig. 4a). In the hippocampus, 69 DEGs from old post-surgical mice and 42 genes from young mice overlapped with DAM, with 11 overlapping between young and old mice (Fig. 4a). Interestingly, a comparison of fold change values showed that most genes upregulated by surgery were downregulated in DAM cells (e.g., *Runx1* for both hemisphere and hippocampus of old and young mice; Fig. 4b and c) whereas genes downregulated by surgery tended to be downregulated in DAM as well (e.g., *Tgfb1*, *olfml3;* Fig. 4b and c). Comparison of post-surgical DEGs with MGnD genes reveals a similar pattern (Fig. S2). In the hemisphere, 85 post-surgery microglial DEGs in the old mice and 19 in the young (15 of which are present in both ages) also appear in the MGnD profile. In the hippocampus, 52 DEGs from the old and 38 from the young overlapped with MGnD genes (Figs. S2a and b). Moreover, surgery decreased expression of MGnD markers such as *Clec7a* in the microglia of old animals (Fig. S2b).

Impact of Apoe

Previous studies using different neurodegenerative mouse models have shown that MGnD microglia are regulated by the reciprocal suppression of TGFβ and induction of APOE signaling [52]. Importantly, targeting microglial APOE signaling restores their homeostatic signature [52, 67]. Because our data indicate that surgery induces the homeostatic phenotype in microglia, we hypothesized that if Apoe is involved, deletion of it would further promote the development of the homeostatic phenotype by surgery. In order to directly investigate this possibility, we exposed old Cx3cr1$^{creERT2/+}$:*Apoe*$^{fl/fl}$ (Apoe cKO) and their age-matched controls to surgery as described above and measured the level of *Apoe*, *Il6,* and the MGnD marker *Clec7a* in microglia by qPCR 6 h after surgery. As expected, tamoxifen treated Cx3cr1^{creERT2}:*Apoe*$^{fl/fl}$ (Apoe cKO) mice had markedly reduced the expression of *Apoe* in microglia compared to the control mice (Fig. S3a) but surgery produced no change in *Apoe* (Fig. S3a). *Clec7a* was reduced by surgery in old control mice (Fig. S3b), which replicates our results in old C57BL/6 mice, and there was a similar trend in the *Apoe* cKO mice, but it did not reach significance. Notably, however, knockout of *Apoe* had no effect on surgery-induced changes in microglial expression of *Il6 or Clec7a* (Fig. S3b, c). This suggests that *Apoe* may not be responsible for the shift in microglia from an MGnD to a homeostatic phenotype after surgery but we cannot exclude the possibility that

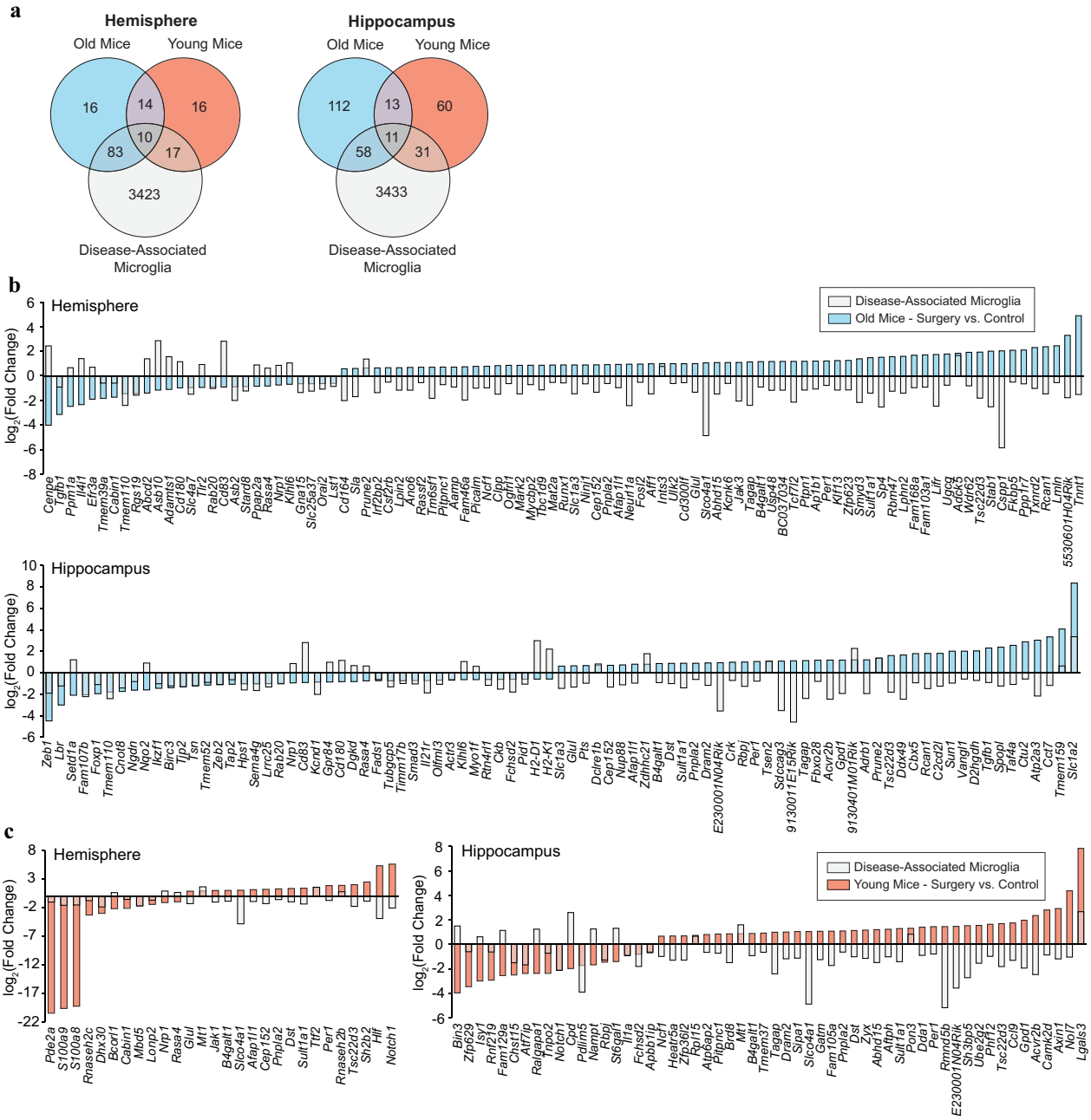

Fig. 4 Overlap of DEGs with profile of DAM. **a** The number of DEGs affected by surgery among old mice and young mice, in the hemisphere and hippocampus, that overlap with genes associated with DAM. **b** Comparison of fold changes for DEGs that overlap with DAM in the hemisphere and hippocampus of old mice. **c** Comparison of fold changes for DEGs that overlap with DAM in the hemisphere and hippocampus of young mice

Apoe secreted by other CNS cells continued to regulate microglial function [68].

Discussion

These experiments demonstrate that microglia in the brain of old mice develop a hypoactive, homeostatic molecular profile (signature) following abdominal surgery and general anesthesia, rather than an activated one. This occurred in concert with a robust surgery-induced systemic inflammatory response in both age groups, evidenced by increases in plasma IL-6 and CCL2 and an acute and persistent increase in CCL2 in the hippocampus of old animals. However, we observed no post-surgical changes in the number or morphology

of Iba1$^+$ cells, a commonly used but non-specific proxy for microglial activation that has been observed in some previous studies of surgery in rodent models [20, 22, 69, 70]. In contrast, our data demonstrate that at the transcriptome level microglia are changed by surgery, albeit in a transient and unexpected way. Surgery modified the microglial transcriptome in both age groups but affected more genes in these cells in old animals. Specifically, the expression of many inflammation-related genes decreased, whereas expression of genes involved in homeostatic or anti-inflammatory functions increased. Pathway analyses revealed a similar pattern, with enhancement of some proinflammatory pathways and suppression of others. Of note, the expression of Clec7a, a major DAM/MGnD gene that is upregulated in multiple mouse models of neurodegeneration and is critical for the debris clearing phagocytic function of microglia, was reduced in microglia from old animals 6 h after surgery. Given that microglial expression of Clec7a increases with age, where it is believed to promote the normal phagocytic activity and protective functions of these cells, these data suggest that surgery suppresses the natural role and purpose of microglia in the old brain. This pattern was confirmed when we compared the post-operative gene expression signature of microglia from the old brain to published signatures of the MGnD and DAM phenotypes. Strikingly, compared to their natural expression profile, the expression of many prototypical MGnD/DAM genes was reversed by surgery such that genes typically more highly expressed in microglia of the MGnD/DAM phenotype than homeostatic cells were expressed at lower levels after surgery. The fact that these changes were both region-specific and transient is consistent with observations that microglia are highly dynamic cells with region-specific molecular phenotypes and functions that change quickly depending on the context and cellular microenvironment [71]. Collectively, therefore, it appears that transient hypoactivity and dysregulation characterize the microglial response to surgery in the aging brain at least in the early phase of recovery.

Microglia have been implicated in post-surgical neuroinflammation, defined as an increase in proinflammatory mediators in brain tissue or cerebrospinal fluid, for some time. Early work in preclinical models of orthopedic or abdominal surgery showed increased proinflammatory mediators in the hippocampus, linked this CNS inflammatory response to cognitive impairment, and demonstrated that pharmacologic or genetic interventions that interfere with CNS inflammation attenuate or block the cognitive deficits [12–25]. Increases in various proinflammatory cytokines have likewise been reported in the blood and CSF of humans in association with postoperative cognitive morbidity [26–29, 72]. Due to their roles as the primary immune cells of the brain and a producer of proinflammatory mediators, it has been assumed that microglial activation is responsible for post-surgical CNS inflammation. This assumption stems mainly from data showing an increase in microglial numbers and/or a change in morphology after surgery by immunohistochemical staining for Iba1. Notably, depleting microglia prior to surgery with CSF1R reduces hippocampal concentrations of inflammatory mediators and blunts surgery-induced learning impairment in a mouse tibial fracture model [69]. However, Iba1 labels both microglia and macrophages and is not a reliable marker of microglial activity [47]. Moreover, many of these studies have been done in young mice [44], posing a significant limitation because, as reports from others and our data show, microglia undergo substantial transcriptional and functional changes with age [47, 73]. Furthermore, two studies that investigated the impact of surgery on microglial activity in humans reveal a different pattern. Both used positron emission tomography to measure expression of ^{11}C-labelled translocator protein PBR28, which is primarily but not exclusively expressed by microglia, and demonstrated a marked but transient reduction in microglial activity days to weeks after surgery in the brains of older patients [55, 56]. In addition, the change in brain ^{11}C-PBR28 had no relationship to CSF or plasma biomarkers of inflammation, or to the development of postoperative delirium [55, 56]. Our transcriptomic data provide new, cell-specific molecular evidence supporting the concept that microglia are hypoactive during the early post-surgical phase of recovery and indicate that the response is age-dependent.

Traditionally, microglia have been primarily viewed as detrimental immune effectors in brain injury and disease. According to this perspective, post-surgical microglial activation or hyperactivity would be considered harmful whereas hypoactivity might be seen as potentially beneficial. While it is true that microglia contribute to aging and neurodegeneration via proinflammatory properties and dysregulated phagocytic functions [43, 74], it is now evident that they also play a vital role in normal brain function. For example, they have homeostatic and neuroprotective functions [37, 45, 46, 75, 76] and play critical roles in synapse pruning, CNS tissue maintenance, pathogen defense, and the injury response [41]. Importantly, not all microglia are the same. Recent studies have identified multiple phenotypes, each characterized by a unique molecular signature and function. In general, microglia are classified as homeostatic [59] or neurodegenerative (MGnD) [52], with the latter alternately referred to as disease associated microglia (DAM) [49]. The phenotype is determined by the reciprocal suppression of

transforming growth factor β (TGFβ) and induction of Trem2-ApoE signaling [59, 77]. MGnD microglia are characterized by the upregulation of several molecules related to immune responses, including Trem2, ApoE, AXL receptor Tyrosine Kinase (Axl), Galectin-3 (Lgals3), TYRO protein tyrosine kinase-binding protein (Tyrobp), Integrin Subunit Alpha X (Itgax), and Clec7a. The MGnD/DAM phenotype is detected in mouse models of aging and neurodegenerative diseases including Alzheimer's Disease (AD), amyotrophic lateral sclerosis (ALS), tauopathy, multiple sclerosis, and glaucoma [49, 52, 78–81][. MGnD/DAM appear to have a protective function during neurodegenerative disease such as AD. This protection is partially attributed to acquisition of a pre-MGnD activation state via IFN-γ signaling [82]. Genetic deletion of MGnD genes such as Trem2 or Axl in AD mice produces microglia that are unable to detect, respond to, and compact amyloid β plaques normally [49, 52, 83–85], leading to enhanced pathological changes. Conversely, studies using TREM2-targeting antibodies to stimulate TREM2, which is essential for the 2nd phase of the microglial transition from the homeostatic to MGnD/DAM phenotype, have beneficial effects on reducing pathology and slowing disease progression in MS and AD models [86–89]. Thus, MGnD/DAM cells can have a protective function in some contexts, and an imbalance between the exacerbating and ameliorating features of MGnD/DAM microglia may result in the initiation or exacerbation of neurodegeneration. Boosting MGnD/DAM activity early after injury or in disease can slow or mitigate damage and progression [50]. It is interesting in this context that surgery is followed by a marked decrease in microglial expression of Clec7a, a major MGnD/DAM-related gene. Clec7a is upregulated in aging, multiple mouse models of neurodegeneration, and in active multiple sclerosis lesions in humans, where it is thought to reflect the neuroprotective response of microglia to neuronal injury [90]. As such, the decrease in Clec7a in microglia from the old brain after surgery suggests that surgical trauma reverses and/or antagonizes the MGnD/DAM phenotype that is prevalent in the old brain. The fact that the broader molecular signature of these cells after surgery differs significantly from the signature of MGnD/DAM phenotypes reported previously further supports this premise. Unexpectedly, this effect of surgery does not appear to be Apoe mediated, as conditional knockout of Apoe in microglia did not further decrease *Clec7a* in these cells. Thus, a transitory surgery-induced loss or impairment of the supportive and protective functions of MGnD microglia in the older brain may contribute to, or be an alternate mechanism for, cognitive dysfunction following surgery.

The elevation of CCL2 in the brain postoperatively in our model, at a time when microglia had a hypoactive molecular signature, may appear paradoxical. However, it is important to note that cytokines and chemokines, including CCL2, play roles beyond inflammation and serve as potent modulators of synaptic plasticity, learning and memory, and neuronal networks in both health and disease [91]. Therefore, an increase in CCL2 may signify more than inflammation. In addition, microglia are not the only source of CCL2 in the brain. A variety of other cells express CCL2, including astrocytes, vascular endothelial cells, circulating macrophages that infiltrate the brain, and even neurons. For example, PDGFRbeta cells in the vessel endothelium produce and signal via CCL2 to glutamatergic neurons to increase excitability [92] and neuronally produced CCL2 attracts monocytes into the brain during acute infection [93]. Moreover, depletion of microglia by administering PLX5622, an antagonist of colony stimulating factor-1, does not mitigate LPS-induced sickness behavior or alter expression of brain cytokines [94]. This implies that microglial activation may not be necessary for surgery-induced sickness-like behavior or acute cerebral inflammation.

This work has both strengths and limitations. Chief among the former is inclusion of both young and old animals and investigation of microglia specifically using cell-specific antibodies and FACS, a method 1000 times more sensitive than immunohistochemistry. Another key strength is that we defined the phenotype of cells through a molecular signature. This approach is critical as it allows for an unbiased investigation of the impact of surgery on thousands of genes and different types of microglia. Further, examining two time points enabled us to identify the transient and age-dependent nature of the changes in the molecular signature, although we cannot say how rapidly it resolves. However, there are also limitations. Our results should be considered exploratory as the small sample size restricts our ability to correct for multiple comparisons. Another limitation is that we cannot exclude the possibility that the microglial response varies with the nature and invasiveness of the surgical trauma. No comparative studies of animal models exist in this context but the laparotomy model we used has been shown in previous studies to produce neuroinflammation and cognitive deficits [95–97]. In addition, surgery requires administration of anesthetics and analgesics that might confound the results. Most general anesthetics, including the isoflurane used in this study, are immune suppressants [19]. Nevertheless, preclinical studies demonstrate that surgery under general anesthesia induces CNS inflammation similar in magnitude to

the same procedure under local anesthesia [12–18, 20, 22, 98–104], indicating that anesthesia itself is unlikely to mask the microglial response. In addition, some studies indicate that anesthesia alone has no lingering impact on postoperative cognition in old animals or humans—making its influence on microglia a less compelling question. The meloxicam administered for postoperative pain relief may also have had an impact. Analgesia is necessary after surgery and opioids and non-steroidal agents such as meloxicam are often used for pain relief in animals and humans but both drug classes have anti-inflammatory effects and direct actions on microglia [105–107]. It seems unlikely this pain management regimen would confound the post-surgery molecular signature we identified, however, because control mice received the same dose of meloxicam. Lastly, the functional significance of the postoperative transcriptomic changes is unclear as the molecular signature is a strong predictor, but not a definitive index, of microglial function. Yet, the fact that microglia have lower Clec7a, a key driver of microglial phagocytosis, and less of a MGnD/DAM phenotype after surgery strongly supports the possibility of a functional correlate for the molecular signature we identified.

Here we demonstrate in an animal model that surgery induces an age-dependent and transient shift in the molecular signature of microglia from the MGnD/DAM type common in the older brain to a homeostatic phenotype. This suggests that in the older brain these cells become less, rather than more, active in the early postoperative period and, as homeostatic microglia are less responsive to damage signals, implies that the ability of microglia to patrol and protect the microenvironment of the brain is compromised during this interval. Whether this microglial state increases vulnerability of the old brain to postoperative cognitive impairment is yet to be determined but our findings challenge the prevailing view that microglia are activated by surgery.

Abbreviations

ELISA	Enzyme-linked immunosorbent assay
FACS	Fluorescence-activated cell sorting
qPCR	Quantitative polymerase chain reaction
RNA-seq	RNA sequencing
DEG	Differentially expressed genes
DAM	Disease-associated microglia
MGnD	Neurodegenerative microglia
IACUC	Institutional Animal Care and Use Committee
BWH	Brigham and Women's Hospital
PBS	Phosphate-buffered saline
T-per	Tissue protein extraction reagent
ROI	Region of interest
DG	Dentate gyrus
IPA	Ingenuity pathway analysis
Nfkb2	Nuclear factor kappa B subunit 2
RelB	RELB proto-oncogene
Il6st	Pro-inflammatory cytokine interleukin-6 signal transducer
Scos3	Suppressor of cytokine signaling 3
Ddit4	DNA damage-inducible transcript 4
ROS	Reactive oxygen species
HMGB1	High mobility group box 1
STAT3	Signal transducer and activator of transcription 3
APOE	Apolipoprotein E
TGFb	Transforming growth factor beta
Runx1	Runt-related transcription factor 1
IHC	Immunohistochemistry
Clec7a	C-type lectin-like domain containing 7A
IL1b	Interleukin 1 beta
IL6	Interleukin 6
Tgfbr1	Transforming growth factor-bete receptor type 1
Tgfb1	Transforming growth factor beta-1
NF-kb	Nuclear factor kb
Igfr1	Insulin like growth factor 1 receptor
Fgf	Fibroblast growth factor
P2ry12	Purinergic Receptor P2Y12
Ccl2	CC motif chemokine ligand 2
OCT	Optimal cutting temperature
HBSS	Hanks' Balanced Salt Solution

Supplementary Information

The online version contains supplementary material available at https://doi.org/10.1186/s12974-024-03307-0.

Additional file 1

Acknowledgements

We thank Rajesh Krishnan (Ann Romney Center for Neurologic Diseases Flow Cytometry Core facility); Brian Tilton (Boston University Medical Center Flow Cytometry Core) for FACS sorting; and the Broad Institute of MIT and Harvard for Smartseq2 RNAseq.

Author contributions

ZY: conception, design, data acquisition, analysis, interpretation, drafting and revising. AL: design, data acquisition, analysis, interpretation, drafting and revising. CP: data acquisition, analysis. ZX, DJC, OB: conception, design. SS: data acquisition, analysis. GC: conception, design, analysis, interpretation, drafting and revising. All authors read and approved the final manuscript.

Funding

This work was funded by NIH Grant 5R01AG051812 to G.C. and O.B. This study was supported by R01GM132668 and R56AG055833 (D.J.C); R21AG061696 (G.C.); R01AG071741 (G.C. and D.J.C.; RF1AG070761 (Z.X); and the Cure Alzheimer Fund, BrightFocus Foundation 2020A016806, R01AG054672, R01AG075509, R21AG076982, NIH/NEIR01 EY027921, NIH/NINDS R01NS088137, R21NS104609, R21NS101673, R01GM132668, and a Nancy Davis Foundation innovative Award (O.B.).

Availability of data and materials

The data that support the findings of this study are available in this manuscript and supplementary information. All relevant data have be deposited into Gene Expression Omnibus (GEO).

Declarations

Ethics approval and consent to participate

The animal use procedures described in this paper were designed according to guidelines provided by the Brigham and Women's Hospital Center for Comparative Medicine and approved by the Institutional Animal Care and Use Committee at Brigham and Women's Hospital.

Consent for publication

Not applicable.

Competing interests

OB: collaboration with GSK, Regulus Therapeutics. Research funding from Sanofi, GSK, honoraria for lectures, consultancy: UCB, Camp4, Ono Pharma USA, General Biophysics. ZX: provided consulting service to Baxter,

NanoMosaic, Shanghai 4th, 9th and 10th hospitals, Shanghai Mental Health Center, and < < Anesthesiology and Perioperative Science > > in last 36 months. DJC is an Executive Editor of Anesthesiology and GC is a Section Editor of Frontiers in Anesthesiology.

Author details
[1]Department of Neurology, Brigham and Women's Hospital, Boston, MA, USA. [2]Department of Ophthalmology, Mass Eye and Ear, Harvard Medical School, Boston, MA, USA. [3]Department of Anesthesiology, Perioperative and Pain Medicine, Brigham and Women's Hospital, Boston, MA, USA. [4]Department of Anesthesia, Critical Care and Pain Medicine, Massachusetts General Hospital, Boston, MA, USA. [5]Department of Anaesthesia, Harvard Medical School, Boston, MA, USA. [6]Department of Anesthesiology and Critical Care, Perelman School of Medicine, University of Pennsylvania, Philadelphia, PA, USA. [7]Evergrande Center for Immunologic Diseases, SchoolBrigham and Women's Hospital, Harvard Medical School, Boston, MA, USA.

Received: 22 March 2024 Accepted: 19 November 2024
Published online: 18 December 2024

References

1. Finlayson EV, Birkmeyer JD. Operative mortality with elective surgery in older adults. Eff Clin Pract. 2001;4(4):172–7.
2. Finlayson E, Wang L, Landefeld CS, Dudley RA. Major abdominal surgery in nursing home residents: a national study. Ann Surg. 2011;254(6):921–6.
3. Chow WB, Rosenthal RA, Merkow RP, Ko CY, Esnaola NF, Program ACoSNSQI, et al. Optimal preoperative assessment of the geriatric surgical patient: a best practices guideline from the American College of Surgeons National Surgical Quality Improvement Program and the American Geriatrics Society. J Am Coll Surg 2012;215: 453-66.
4. Saczynski JS, Marcantonio ER, Quach L, Fong TG, Gross A, Inouye SK, et al. Cognitive trajectories after postoperative delirium. N Engl J Med. 2012;367(1):30–9.
5. Gross AL, Jones RN, Habtemariam DA, Fong TG, Tommet D, Quach L, et al. Delirium and long-term cognitive trajectory among persons with dementia. Arch Intern Med. 2012;172(17):1324–31.
6. Fong TG, Jones RN, Shi P, Marcantonio ER, Yap L, Rudolph JL, et al. Delirium accelerates cognitive decline in Alzheimer disease. Neurology. 2009;72(18):1570–5.
7. Pandharipande PP, Girard TD, Jackson JC, Morandi A, Thompson JL, Pun BT, et al. Long-term cognitive impairment after critical illness. N Engl J Med. 2013;369(14):1306–16.
8. Gleason LJ, Schmitt EM, Kosar CM, Tabloski P, Saczynski JS, Robinson T, et al. Effect of delirium and other major complications on outcomes after elective surgery in older adults. JAMA Surg. 2015;150:1134–40.
9. Yang T, Velagapudi R, Terrando N. Neuroinflammation after surgery: from mechanisms to therapeutic targets. Nat Immunol. 2020;21(11):1319–26.
10. Rosas-Ballina M, Tracey KJ. The neurology of the immune system: neural reflexes regulate immunity. Neuron. 2009;64(1):28–32.
11. Weber MD, Frank MG, Tracey KJ, Watkins LR, Maier SF. Stress induces the danger-associated molecular pattern HMGB-1 in the hippocampus of male Sprague Dawley rats: a priming stimulus of microglia and the NLRP3 inflammasome. J Neurosci. 2015;35(1):316–24.
12. Wan Y, Xu J, Ma D, Zeng Y, Cibelli M, Maze M. Postoperative impairment of cognitive function in rats: a possible role for cytokine-mediated inflammation in the hippocampus. Anesthesiology. 2007;106(3):436–43.
13. Cibelli M, Fidalgo AR, Terrando N, Ma D, Monaco C, Feldmann M, et al. Role of interleukin-1beta in postoperative cognitive dysfunction. Ann Neurol. 2010;68(3):360–8.
14. Fidalgo AR, Cibelli M, White JPM, Nagy I, Maze M, Ma D. Systemic inflammation enhances surgery-induced cognitive dysfunction in mice. Neurosci Lett. 2011;498(1):63–6.
15. Fidalgo AR, Cibelli M, White JPM, Nagy I, Noormohamed F, Benzonana L, et al. Peripheral orthopaedic surgery down-regulates hippocampal brain-derived neurotrophic factor and impairs remote memory in mouse. Neuroscience. 2011;190:194–9.
16. He HJ, Wang Y, Le Y, Duan KM, Yan XB, Liao Q, et al. Surgery upregulates high mobility group box-1 and disrupts the blood-brain barrier causing cognitive dysfunction in aged rats. CNS Neurosci Ther. 2012;18(12):994–1002.
17. Terrando N, Monaco C, Ma D, Foxwell BM, Feldmann M, Maze M. Tumor necrosis factor-alpha triggers a cytokine cascade yielding postoperative cognitive decline. Proc Natl Acad Sci USA. 2010;107(47):20518–22.
18. Feng X, Degos V, Koch LG, Britton SL, Zhu Y, Vacas S, et al. Surgery results in exaggerated and persistent cognitive decline in a rat model of the Metabolic Syndrome. Anesthesiology. 2013;118(5):1098–105.
19. Tang JX, Mardini F, Janik LS, Garrity ST, Li RQ, Bachlani G, et al. Modulation of murine Alzheimer pathogenesis and behavior by surgery. Ann Surg. 2013;257(3):439–48.
20. Hovens IB, Schoemaker RG, van der Zee EA, Heineman E, Nyakas C, van Leeuwen BL. Surgery-induced behavioral changes in aged rats. Exp Gerontol. 2013;48(11):1204–11.
21. Le Y, Liu S, Peng M, Tan C, Liao Q, Duan K, et al. Aging differentially affects the loss of neuronal dendritic spine, neuroinflammation and memory impairment at rats after surgery. PLoS ONE. 2014;9(9): e106837.
22. Hovens IB, van Leeuwen BL, Nyakas C, Heineman E, van der Zee EA, Schoemaker RG. Postoperative cognitive dysfunction and microglial activation in associated brain regions in old rats. Neurobiol Learn Mem. 2015;118:74–9.
23. Terrando N, Rei Fidalgo A, Vizcaychipi M, Cibelli M, Ma D, Monaco C, et al. The impact of IL-1 modulation on the development of lipopolysaccharide-induced cognitive dysfunction. Crit Care. 2010;14(3):R88.
24. Terrando N, Eriksson LI, Ryu JK, Yang T, Monaco C, Feldmann M, et al. Resolving postoperative neuroinflammation and cognitive decline. Ann Neurol. 2011;70(6):986–95.
25. Terrando N, Gomez-Galan M, Yang T, Carlstrom M, Gustavsson D, Harding RE, et al. Aspirin-triggered resolvin D1 prevents surgery-induced cognitive decline. FASEB J. 2013;27(9):3564–71.
26. Vasunilashorn SM, Ngo LH, Dillon ST, Fong TG, Carlyle BC, Kivisäkk P, et al. Plasma and cerebrospinal fluid inflammation and the blood-brain barrier in older surgical patients: the Role of Inflammation after Surgery for Elders (RISE) study. J Neuroinflammation. 2021;18(1):103.
27. Vasunilashorn SM, Dillon ST, Chan NY, Fong TG, Joseph M, Tripp B, et al. Proteome-Wide Analysis using SOMAscan Identifies and Validates Chitinase-3-Like Protein 1 as a Risk and Disease Marker of Delirium Among Older Adults Undergoing Major Elective Surgery. J Gerontol A Biol Sci Med Sci. 2021;77:484–93.
28. VanDusen KW, Li Y-J, Cai V, Hall A, Hiles S, Thompson JW, et al. Cerebrospinal fluid proteome changes in older non-cardiac surgical patients with postoperative cognitive dysfunction. J Alzheimer's Dis. 2021;80(3):1281–97.
29. Oren RL, Kim EJ, Leonard AK, Rosner B, Chibnik LB, Das S, et al. Age-dependent differences and similarities in the plasma proteomic signature of postoperative delirium. Sci Rep. 2023;13(1):7431.
30. Streit WJ, Miller KR, Lopes KO, Njie E. Microglial degeneration in the aging brain–bad news for neurons? Front Biosci. 2008;13:3423–38.
31. Mildner A, Schlevogt B, Kierdorf K, Bottcher C, Erny D, Kummer MP, et al. Distinct and non-redundant roles of microglia and myeloid subsets in mouse models of Alzheimer's disease. J Neurosci. 2011;31(31):11159–71.
32. Krabbe G, Halle A, Matyash V, Rinnenthal JL, Eom GD, Bernhardt U, et al. Functional impairment of microglia coincides with Beta-amyloid deposition in mice with Alzheimer-like pathology. PLoS ONE. 2013;8(4): e60921.
33. Griciuc A, Serrano-Pozo A, Parrado AR, Lesinski AN, Asselin CN, Mullin K, et al. Alzheimer's disease risk gene CD33 inhibits microglial uptake of amyloid beta. Neuron. 2013;78(4):631–43.
34. Bruck W, Porada P, Poser S, Rieckmann P, Hanefeld F, Kretzschmar HA, et al. Monocyte/macrophage differentiation in early multiple sclerosis lesions. Ann Neurol. 1995;38(5):788–96.
35. Li H, Newcombe J, Groome NP, Cuzner ML. Characterization and distribution of phagocytic macrophages in multiple sclerosis plaques. Neuropathol Appl Neurobiol. 1993;19(3):214–23.
36. Derecki NC, Cronk JC, Lu Z, Xu E, Abbott SBG, Guyenet PG, et al. Wild-type microglia arrest pathology in a mouse model of Rett syndrome. Nature. 2012;484(7392):105–9.

37. Prinz M, Priller J. Microglia and brain macrophages in the molecular age: from origin to neuropsychiatric disease. Nat Rev Neurosci. 2014;15(5):300–12.
38. Consortium TNaPASotPG, (IIBDGC) IIBDGC, IIBDGC IIBDGC. Psychiatric genome-wide association study analyses implicate neuronal, immune and histone pathways. Nat Neurosci. 2015.
39. Monk TG, Weldon BC, Garvan CW, Dede DE, van der Aa MT, Heilman KM, et al. Predictors of cognitive dysfunction after major noncardiac surgery. Anesthesiology. 2008;108(1):18–30.
40. Yamasaki R, Lu H, Butovsky O, Ohno N, Rietsch AM, Cialic R, et al. Differential roles of microglia and monocytes in the inflamed central nervous system. J Exp Med. 2014;211(8):1533–49.
41. Colonna M, Butovsky O. Microglia function in the central nervous system during health and neurodegeneration. Annu Rev Immunol. 2017;35(1):441–68.
42. Butovsky O, Weiner HL. Microglial signatures and their role in health and disease. Nat Rev Neurosci. 2018;19(10):622–35.
43. Heneka MT, Carson MJ, El Khoury J, Landreth GE, Brosseron F, Feinstein DL, et al. Neuroinflammation in Alzheimer's disease. Lancet Neurol. 2015;14(4):388–405.
44. Guo LY, Kaustov L, Brenna CTA, Patel V, Zhang C, Choi S, et al. Cognitive deficits after general anaesthesia in animal models: a scoping review. Br J Anaesth. 2022;30:e351–60.
45. Ransohoff RM, Cardona AE. The myeloid cells of the central nervous system parenchyma. Nature. 2010;468(7321):253–62.
46. Prinz M, Priller J, Sisodia SS, Ransohoff RM. Heterogeneity of CNS myeloid cells and their roles in neurodegeneration. Nat Neurosci. 2011;14(10):1227–35.
47. Paolicelli RC, Sierra A, Stevens B, Tremblay M-E, Aguzzi A, Ajami B, et al. Microglia states and nomenclature: a field at its crossroads. Neuron. 2022;110(21):3458–83.
48. Masuda T, Sankowski R, Staszewski O, Prinz M. Microglia Heterogeneity in the Single-Cell Era. Cell Rep. 2020;30(5):1271–81.
49. Keren-Shaul H, Spinrad A, Weiner A, Matcovitch-Natan O, Dvir-Szternfeld R, Ulland TK, et al. A unique microglia type associated with restricting development of Alzheimer's disease. Cell. 2017;169(7):1276-90.e17.
50. Deczkowska A, Keren-Shaul H, Weiner A, Colonna M, Schwartz M, Amit I. Disease-associated microglia: a universal immune sensor of neurodegeneration. Cell. 2018;173(5):1073–81.
51. Sala Frigerio C, Wolfs L, Fattorelli N, Thrupp N, Voytyuk I, Schmidt I, et al. The Major Risk Factors for Alzheimer's Disease: Age, Sex, and Genes Modulate the Microglia Response to Aβ Plaques. Cell Rep. 2019;27(4):1293-306.e6.
52. Krasemann S, Madore C, Cialic R, Baufeld C, Calcagno N, El Fatimy R, et al. The TREM2-APOE Pathway Drives the Transcriptional Phenotype of Dysfunctional Microglia in Neurodegenerative Diseases. Immunity. 2017;47(3):566–81 e9.
53. Rosczyk HA, Sparkman NL, Johnson RW. Neuroinflammation and cognitive function in aged mice following minor surgery. Exp Gerontol. 2008;43(9):840–6.
54. Mardini F, Tang JX, Li JC, Arroliga MJ, Eckenhoff RG, Eckenhoff MF. Effects of propofol and surgery on neuropathology and cognition in the 3xTgAD Alzheimer transgenic mouse model. Br J Anaesth. 2017;119(3):472–80.
55. Forsberg A, Cervenka S, Jonsson Fagerlund M, Rasmussen LS, Zetterberg H, Erlandsson Harris H, et al. The immune response of the human brain to abdominal surgery. Ann Neurol. 2017;81(4):572–82.
56. Katsumi Y, Racine AM, Torrado-Carvajal A, Loggia ML, Hooker JM, Greve DN, et al. The Role of Inflammation after Surgery for Elders (RISE) study_ Examination of [11C]PBR28 binding and exploration of its link to postoperative delirium. Neuroimage Clin. 2020;27: 102346.
57. Parkhurst CN, Yang G, Ninan I, Savas JN, Yates JR, Lafaille JJ, et al. Microglia Promote Learning-Dependent Synapse Formation through Brain-Derived Neurotrophic Factor. Cell. 2013;155(7):1596–609.
58. Wagner T, Bartelt A, Schlein C, Heeren J. Genetic Dissection of Tissue-Specific Apolipoprotein E Function for Hypercholesterolemia and Diet-Induced Obesity. PLoS ONE. 2015;10(12): e0145102.
59. Butovsky O, Jedrychowski MP, Moore CS, Cialic R, Lanser AJ, Gabriely G, et al. Identification of a unique TGF-beta-dependent molecular and functional signature in microglia. Nat Neurosci. 2014;17(1):131–43.
60. Picelli S, Bjorklund AK, Faridani OR, Sagasser S, Winberg G, Sandberg R. Smart-seq2 for sensitive full-length transcriptome profiling in single cells. Nat Methods. 2013;10(11):1096–8.
61. Zhang Y, Park C, Bennett C, Thornton M, Kim D. Rapid and accurate alignment of nucleotide conversion sequencing reads with HISAT-3N. Genome Res. 2021;31(7):1290–5.
62. Patro R, Duggal G, Love MI, Irizarry RA, Kingsford C. Salmon provides fast and bias-aware quantification of transcript expression. Nat Methods. 2017;14(4):417–9.
63. Ewels P, Magnusson M, Lundin S, Kaller M. MultiQC: summarize analysis results for multiple tools and samples in a single report. Bioinformatics. 2016;32(19):3047–8.
64. Jie Z, Ko CJ, Wang H, Xie X, Li Y, Gu M, et al. Microglia promote autoimmune inflammation via the noncanonical NF-kappaB pathway. Sci Adv. 2021;7(36):eabh0609.
65. Lopez-Gonzalez I, Schluter A, Aso E, Garcia-Esparcia P, Ansoleaga B, F LL, et al. Neuroinflammatory signals in Alzheimer disease and APP/PS1 transgenic mice: correlations with plaques, tangles, and oligomeric species. J Neuropathol Exp Neurol. 2015;74(4):319–44.
66. Chakrabarti S, Jana M, Roy A, Pahan K. Upregulation of Suppressor of Cytokine Signaling 3 in Microglia by Cinnamic Acid. Curr Alzheimer Res. 2018;15(10):894–904.
67. Shi Y, Yamada K, Liddelow SA, Smith ST, Zhao L, Luo W, et al. ApoE4 markedly exacerbates tau-mediated neurodegeneration in a mouse model of tauopathy. Nature. 2017;549(7673):523–7.
68. Blumenfeld J, Yip O, Kim MJ, Huang Y. Cell type-specific roles of APOE4 in Alzheimer disease. Nat Rev Neurosci. 2024;25(2):91–110.
69. Feng X, Valdearcos M, Uchida Y, Lutrin D, Maze M, Koliwad SK. Microglia mediate postoperative hippocampal inflammation and cognitive decline in mice. JCI Insight. 2017;2(7):1–12.
70. Hu J, Feng X, Valdearcos M, Lutrin D, Uchida Y, Koliwad SK, et al. Interleukin-6 is both necessary and sufficient to produce perioperative neurocognitive disorder in mice. Br J Anaesth. 2018;120(3):537–45.
71. Grabert K, Michoel T, Karavolos MH, Clohisey S, Baillie JK, Stevens MP, et al. Microglial brain region-dependent diversity and selective regional sensitivities to aging. Nat Neurosci. 2016;19(3):504–16.
72. Berger M, Browndyke JN, Wright MC, Nobuhara C, Reese M, Acker L, et al. Postoperative changes in cognition and cerebrospinal fluid neurodegenerative disease biomarkers. Ann Clin Transl Neurol. 2022;9:155–70.
73. Angelova DM, Brown DR. Microglia and the aging brain: Are senescent microglia the key to neurodegeneration? J Neurochem. 2019;151(6):676–88.
74. Hickman S, Izzy S, Sen P, Morsett L, El Khoury J. Microglia in neurodegeneration. Nat Neurosci. 2018;21(10):1359–69.
75. Blank T, Goldmann T, Prinz M. Microglia fuel the learning brain. Trends Immunol. 2014;35(4):139–40.
76. Benarroch EE. Microglia: Multiple roles in surveillance, circuit shaping, and response to injury. Neurology. 2013;81(12):1079–88.
77. Gosselin D, Link VM, Romanoski CE, Fonseca GJ, Eichenfield DZ, Spann NJ, et al. Environment drives selection and function of enhancers controlling tissue-specific macrophage identities. Cell. 2014;159(6):1327–40.
78. Hickman SE, Kingery ND, Ohsumi TK, Borowsky ML, Wang L-C, Means TK, et al. The microglial sensome revealed by direct RNA sequencing. Nat Neurosci. 2013;16(12):1896–905.
79. Holtman IR, Raj DD, Miller JA, Schaafsma W, Yin Z, Brouwer N, et al. Induction of a common microglia gene expression signature by aging and neurodegenerative conditions: a co-expression meta-analysis. Acta Neuropathol Commun. 2015;3(1):31.
80. Zhai Q, Li F, Chen X, Jia J, Sun S, Zhou D, Ma L, Jiang T, Bai F, Xiong L, Wang Q. Triggering Receptor Expressed on Myeloid Cells 2, a Novel Regulator of Immunocyte Phenotypes Confers Neuroprotection by Relieving Neuroinflammation. Anesthesiology. 2017;127:98–110.
81. Margeta MA, Yin Z, Madore C, Pitts KM, Letcher SM, Tang J, et al. Apolipoprotein E4 impairs the response of neurodegenerative retinal microglia and prevents neuronal loss in glaucoma. Immunity. 2022;55(9):1627-44.e7.
82. Yin Z, Herron S, Silveira S, Kleemann K, Gauthier C, Mallah D, et al. Identification of a protective microglial state mediated by miR-155 and interferon-gamma signaling in a mouse model of Alzheimer's disease. Nat Neurosci. 2023;26(7):1196–207.

83. Wang Y, Ulland TK, Ulrich JD, Song W, Tzaferis JA, Hole JT, et al. TREM2-mediated early microglial response limits diffusion and toxicity of amyloid plaques. J Exp Med. 2016;213(5):667–75.
84. Huang Y, Happonen KE, Burrola PG, O'Connor C, Hah N, Huang L, et al. Microglia use TAM receptors to detect and engulf amyloid β plaques. Nat Immunol. 2021;22(5):586–94.
85. Yuan P, Condello C, Keene CD, Wang Y, Bird TD, Paul SM, et al. TREM2 haplodeficiency in mice and humans impairs the microglia barrier function leading to decreased amyloid compaction and severe axonal dystrophy. Neuron. 2016;92(1):252–64.
86. Ellwanger DC, Wang S, Brioschi S, Shao Z, Green L, Case R, et al. Prior activation state shapes the microglia response to antihuman TREM2 in a mouse model of Alzheimer's disease. Proc Natl Acad Sci USA. 2021;118(3): e2017742118.
87. Cignarella F, Filipello F, Bollman B, Cantoni C, Locca A, Mikesell R, et al. TREM2 activation on microglia promotes myelin debris clearance and remyelination in a model of multiple sclerosis. Acta Neuropathol. 2020;140(4):513–34.
88. Schlepckow K, Monroe KM, Kleinberger G, Cantuti-Castelvetri L, Parhizkar S, Xia D, et al. Enhancing protective microglial activities with a dual function TREM2 antibody to the stalk region. EMBO Mol Med. 2020;12(4): e11227.
89. Fassler M, Rappaport MS, Cuno CB, George J. Engagement of TREM2 by a novel monoclonal antibody induces activation of microglia and improves cognitive function in Alzheimer's disease models. J Neuroinflammation. 2021;18(1):19.
90. Deerhake ME, Shinohara ML. Emerging roles of Dectin-1 in noninfectious settings and in the CNS. Trends Immunol. 2021;42(10):891–903.
91. Zipp F, Bittner S, Schafer DP. Cytokines as emerging regulators of central nervous system synapses. Immunity. 2023;56(5):914–25.
92. Duan L, Zhang X-D, Miao W-Y, Sun Y-J, Xiong G, Wu Q, et al. PDGFRβ cells rapidly relay inflammatory signal from the circulatory system to neurons via chemokine CCL2. Neuron. 2018;100(1):183-200.e8.
93. Howe CL, LaFrance-Corey RG, Goddery EN, Johnson RK, Mirchia K. Neuronal CCL2 expression drives inflammatory monocyte infiltration into the brain during acute virus infection. J Neuroinflammation. 2017;14(1):238–314.
94. Vichaya EG, Malik S, Sominsky L, Ford BG, Spencer SJ, Dantzer R. Microglia depletion fails to abrogate inflammation-induced sickness in mice and rats. J Neuroinflammation. 2020;17(1):172.
95. Zhao L, Wang F, Gui B, Hua F, Qian Y. Prophylactic lithium alleviates postoperative cognition impairment by phosphorylating hippocampal glycogen synthase kinase-3β (Ser9) in aged rats. Exp Gerontol. 2011;46(12):1031–6.
96. Age-dependent postoperative cognitive impairment and Alzheimer-related neuropathology in mice., (2014).
97. Yang S, Gu C, Mandeville ET, Dong Y, Esposito E, Zhang Y, et al. Anesthesia and Surgery Impair Blood-Brain Barrier and Cognitive Function in Mice. Front Immunol. 2017;8:902.
98. Hovens IB, Schoemaker RG, van der Zee EA, Absalom AR, Heineman E, van Leeuwen BL. Postoperative cognitive dysfunction: Involvement of neuroinflammation and neuronal functioning. Brain Behav Immun. 2014;38:202–10.
99. Kim J-A, Li L, Zuo Z. Delayed treatment with isoflurane attenuates lipopolysaccharide and interferon gamma-induced activation and injury of mouse microglial cells. Anesthesiology. 2009;111(3):566–73.
100. Luo T, Wu J, Kabadi SV, Sabirzhanov B, Guanciale K, Hanscom M, et al. Propofol limits microglial activation after experimental brain trauma through inhibition of nicotinamide adenine dinucleotide phosphate oxidase. Anesthesiology. 2013;119(6):1370–88.
101. Ye X, Lian Q, Eckenhoff MF, Eckenhoff RG, Pan JZ. Differential general anesthetic effects on microglial cytokine expression. PLoS ONE. 2013;8(1): e52887.
102. Tanaka T, Kai S, Matsuyama T, Adachi T, Fukuda K, Hirota K. General anesthetics inhibit LPS-induced IL-1β expression in glial cells. PLoS ONE. 2013;8(12): e82930.
103. Peng M, Ye JS, Wang YL, Chen C, Wang CY. Posttreatment with propofol attenuates lipopolysaccharide-induced up-regulation of inflammatory molecules in primary microglia. Inflamm Res Off J Eur Hist Res Soc [et al]. 2014;63(5):411–8.
104. Wu X, Lu Y, Dong Y, Zhang G, Zhang Y, Xu Z, et al. The inhalation anesthetic isoflurane increases levels of proinflammatory TNF-α, IL-6, and IL-1β. Neurobiol Aging. 2012;33(7):1364–78.
105. Fiebich BL, Biber K, Lieb K, van Calker D, Berger M, Bauer J, et al. Cyclooxygenase-2 expression in rat microglia is induced by adenosine A2a-receptors. Glia. 1996;18(2):152–60.
106. Peng J, Pan J, Wang H, Mo J, Lan L, Peng Y. Morphine-induced microglial immunosuppression via activation of insufficient mitophagy regulated by NLRX1. J Neuroinflammation. 2022;19(1):87.
107. King'uyu DN, Nti-Kyemereh L, Bonin JL, Feustel PJ, Tram M, MacNamara KC, et al. The effect of morphine on rat microglial phagocytic activity: an in vitro study of brain region-, plating density-, sex-, morphine concentration-, and receptor-dependency. J Neuroimmunol. 2023;384: 578204.

Publisher's Note